China Ocean Eng., 2018, Vol. 32, No. 3, P. 278–287
DOI: https://doi.org/ 10.1007/s13344-018-0029-6, ISSN 0890-5487
http://www.chinaoceanengin.cn/ E-mail: coe@nhri.cn

Numerical Simulation of Sloshing Using the MPS-FSI Method with Large Eddy Simulation

YANG Chao[a, b], ZHANG Huai-xin[a, b, *], SU Hui-lin[c], SHEN Zhong-xiang[d]

[a]State Key Laboratory of Ocean Engineering, School of Naval Architecture, Ocean and Civil Engineering, Shanghai Jiao Tong University, Shanghai 200240, China

[b]Collaborative Innovation Center for Advanced Ship and Deep-Sea Exploration (CISSE), Shanghai Jiao Tong University, Shanghai 200240, China

[c]PLA Army Engineering University, Nanjing 210007, China

[d]School of Naval Architecture and Ocean Engineering, Dalian Maritime University, Dalian 116026, China

Received June 29, 2017; revised March 19, 2018; accepted March 27, 2018

Abstract

A numerical model has been developed to study sloshing of turbulent flow in a tank with elastic baffles. The Moving-Particle Semi-implicit method (MPS) is a kind of meshless Lagrangian calculation method. The large eddy simulation (LES) approach is employed to model the turbulence by using the Smagorinsky Sub-Particle Scale (SPS) closure model. This paper uses MPS-FSI method with LES to simulate the interaction between free surface flow and a thin elastic baffle in sloshing. Then, the numerical model is validated, and the numerical solution has good agreement with experimental data for sloshing in a tank with elastic baffles. Furthermore, under external excitations, the MPS is applied to viscous laminar flow and turbulent flow, with both the deformation of elastic baffles and the wave height of the free surface are compared with each other. Besides, the impact pressure with/without baffles and wave height of free surface are investigated and discussed in detail. Finally, preliminary simulations are carried out in the damage problem of elastic baffles, taking the advantage of the MPS-FSI method in computations of the fluid–structure interaction with large deformation.

Key words: moving particle semi-implicit method (MPS), fluid–structure interaction (FSI), large eddy simulation (LES), meshless, sloshing

Citation: Yang, C., Zhang, H. X., Su, H. L., Shen, Z. X., 2018. Numerical simulation of sloshing using the MPS-FSI method with large eddy simulation. China Ocean Eng., 32(3): 278–287, doi: https://doi.org/ 10.1007/s13344-018-0029-6

1 Introduction

It is of significant importance to study the sloshing problem for the safe operation in sailing tanker. The fluid–structure interaction (FSI) in sloshing is especially important to the design of the tanker, the stability and safety of the ship structures. With the increase of the volume of liquid cargo and the large oil tanker, the fluid–structure interaction for sloshing has again attracted attentions from academia and the industry, which becomes an advanced research hotspot in ship hydrodynamics.

The research on sloshing derives from Abramson (1966), who has summarized the linear potential flow theory in the field of Aeronautics and Astronautics in 1950s, and then the corresponding researches really began. With the development of computer technologies, numerous mesh methods have been widely used in the numerical study of sloshing. Kim (2001) simulated sloshing in a rectangle tank based on the finite difference method. Okamoto and Kawahara (1990) conducted simulations on sloshing both in the 2D rectangle tank and the prismatic tank based on finite element method. Nakayama also carried out simulations on sloshing in the 2D rectangle tank. Jung et al. (2008) simulated the interaction between the sloshing impact pressure and the tank structure in the same case as the experiments using MSC.Dytran software. Based on the previous studies, the use of internal baffles is considered to be an effective means on reducing the sloshing amplitude. Cho and Lee (2004) studied numerically the effects of baffle on liquid sloshing in a tank using an FEM model. Biswal et al. (2006) adopted the FEM to investigate the 2D nonlinear sloshing in both rectangular and cylindrical tanks with rigid baffles. But all above are limited to rigid baffles having been studied. In recent years, as the development of science and technology, the numerical simulations of the FSI between the free sur-

Foundation item: This research is financially supported by the National Natural Science Foundation of China (Grant Nos. 51479116 and 11272213).
*Corresponding author. E-mail: huaixinzhang@126.com

face and elastic baffles have been gaining more and more attention. Liao and Hu (2013) successfully simulated the interaction between free surface flow and a thin elastic plate in a sloshing tank by the coupling finite difference method (FDM) and the finite element method (FEM). Dunne and Rannacher (2006) applied a technique similar to the level set method and a mesh adaptation method to solve the FSI problems based on the Eulerian formulation.

Traditional mesh methods have been widely used in various fields of the FSI calculation. However, there are some weaknesses in the mesh numerical methods. For example, when the numerical methods based on grids are used in the simulations of physical problems involved with large deformation, large gradient, moving interface and violent free surface flow etc., the grids need to be reconstructed constantly, which would not only cost a large amount of calculation, but also lead to poor accuracy. The method of meshless—the particle methods developed rapidly in recent years, is more flexible compared with traditional grid methods. Its main idea is to express fluid domain and solid domain using a series of discrete Lagrange particles. Due to rid itself of the constraints of computational grids, completely aside the grid reconstruction, meshless method has a very distinct advantage in dealing with the discontinuous problems of the fluid solid coupling interface and so on.

Smoothed particle hydrodynamics (SPH) is a fully Lagrange particle method. It emerged as the worlds earliest true meshless method, which had significant influence on the follow-up meshless methods. SPH was originally introduced by Gingold and Monaghan (1977) and Lucy (1977) to simulate astrophysical phenomena. Nowadays, SPH also has been used to simulate the FSI problems involved with the free surface flow interaction with a deformable structure. SPH is mainly for the compressible flow calculations. Whereas for incompressible flow, an additional processing is needed to make it artificially compressible. In the SPH method, physical quantities are calculated explicitly. Even though the explicit calculation is simple, it is hard to obtain the correct pressure values, and the time step limited by the speed of sound leads to low computing efficiency.

However, in the MPS method, a new Lagrangian particle method and first proposed by Koshizuka et al. (1995), Koshizuka and Oka (1996), the fluid is truly incompressible. The pressure is calculated implicitly, whereas the viscous force and body force are calculated explicitly. This semi-implicit manner enables the MPS method to accept a larger time step to reduce calculation amount. MPS has enjoyed very extensive applications and been widely applied in many research fields since the advent. In practical engineering problems, many problems related with flowing fluid are turbulent flow, and large eddy simulation (LES) is a major means of research on turbulence. With respect to the ordinary governing equation, sub-particle scale models are added in LES. In 2001, Gotoh et al. (2001), for the first time, applied the large-eddy turbulence model to the MPS method. Pan et al. (2012) carried out research on main problems existing in MPS-LES method. He developed a new technique of the free surface recognition. Based on the MPS-LES method, Yu and Zhang (2013) simulated the impact of a wedge into the water problem. In 2001, Chikazawa et al. (2001) adopted the MPS method in the FSI.

The FSI problems of sloshing in a tank involving large deformations of the free surface and the extreme response of the structure are always hot and difficult spots in ocean engineering. The interface of the FSI problems is the boundary between two different media which differs from the boundary problems in solid mechanics or fluid mechanics. The interaction between fluid and solid mainly happens on the mobile interface and the handle of the interface. Data transformation plays a decisive role in the computational efficiency and results. During the early development of the MPS method, many studies focused on the simulation of fluid, with few studies on fluid–structure coupling problems. This happened because they met problems when they used the MPS method to handle the FSI problems. Firstly, considering MPS method being a full Lagrangian meshless particle method, it always happens that fluid particles cross solid boundary will affect the precision of the numerical calculation. It is always a difficult problem on the MPS method on handling the interface to ensure the precision and efficiency. Secondly, the common disadvantage of MPS method and another meshless method SPH method is that the pressure oscillation is too high. It is hard to reduce the pressure oscillation so as to improve precision. The innovations of this paper are as follows. Firstly, when calculating the FSI problems, both the mesh method and the meshless method generally have a special processing for the interface. However, it is very difficult to handle the interface which always leads to the calculation interrupting. This paper uses a bran-new calculating procedure to simulate the calculation of FSI problems. The calculation process is mainly divided into two steps: first, ignore the properties of the solid particle and treat all particles as fluid particles; second, add the natural attributes to the solid particles and correct the results. The biggest advantage of this method is that it is not necessary to do special processing for the interface in the FSI. It can simplify the calculation program and improve the calculation efficiency. Secondly, an additional correction procedure to prevent fluid particles from passing through solid boundary is added. In the calculation, if the fluid particles are too close to the solid particles, an additional correction is used to keep a right distance between the fluid particles and the solid particles and at the same time the velocity of the particles is also properly corrected. Considering that correcting the velocity of the particle too much may affect the calculation, the correction value takes the sum of the difference in the velocity between the particle and its neighbors. Thirdly, according to the characteristic of

the calculation procedure of the MPS method, a new pressure iteration method in this paper, which reduces the pressure oscillation, is used to solve the pressure Poisson equation. Fourthly, in actual engineering, there are a lot of practical problems which belong to turbulence. Thus, it is meaningful to simulate the FSI problem of sloshing in a tank in turbulence. This paper used LES to study this problem. Fifthly, taking advantage of the dominance of the MPS methods with full Lagrange characteristic to simulate preliminarily the structural damage under extreme conditions of fluid and solid coupling is the next research focus.

In this paper, by numerically simulating the phenomenon of sloshing with elastic baffle in the tank, the results show that the MPS-FSI method with LES can be well applied to the sloshing problems with a consideration of fluid–structure coupling.

2 MPS method

2.1 The governing equations of fluid

The continuity and Navier-Stokes equations are used as the governing equations for incompressible flow:

$$\nabla \cdot \boldsymbol{v} = 0; \tag{1}$$

$$\frac{\mathrm{D}\boldsymbol{v}}{\mathrm{D}t} = -\frac{1}{\rho}\nabla P + \upsilon \nabla^2 \boldsymbol{v} + F. \tag{2}$$

In Eqs. (1) and (2), ρ is the density of fluid, t is the time, $\boldsymbol{v}$ is the velocity vector, P is the pressure, and F is the body forces.

In the MPS method, the relationships of the particles substitute for the differential operators in traditional methods. The kernel function is used for a particle's interaction with others. Kernel function is as follows:

$$w(r) = \begin{cases} \dfrac{r_\mathrm{e}}{r} - 1, & 0 \leqslant r_\mathrm{e} \leqslant r \\ 0, & r_\mathrm{e} \leqslant r \end{cases} \tag{3}$$

where r is the distance between the particle and its neighboring particles, r_e is the radius of the domain of particle i.

Particle number density is defined as follows:

$$n_i = \sum_{j \neq i} w\left(\left|r_i - r_j\right|\right). \tag{4}$$

It is the sum of the kernel functions of one particle i that works with other particles within the range of particle i. Vectors r_i and r_j are the position coordinates of particles i and j.

The discretization of the gradient operator can be expressed as the weighted average of the radial functions. For example, the pressure gradient of particle i can be written as:

$$\langle \nabla p \rangle_i = \frac{D}{n^0} \sum_{j \neq i} \frac{p_j + p_i}{\left|r_j - r_i\right|^2} \left(r_j - r_i\right) w\left(\left|r_j - r_i\right|\right), \tag{5}$$

where the number D is the space dimensions, n^0 is the initial particle number density which can be obtained by Eq. (4) in the initial step of the simulation.

MPS uses the gradient model and Laplacian model to replace terms of the governing equation, which are represented in the following form:

$$< \nabla^2 \Phi >_i = \frac{2D}{\lambda n^0} \sum_{j \neq i} \left[\left(\Phi_j - \Phi_i\right) w\left(\left|r_j - r_i\right|\right)\right] \tag{6}$$

λ in Eq. (6) can be obtained as follows:

$$\lambda = \frac{\sum\limits_{j \neq i} w\left(\left|r_j - r_i\right|\right)\left|r_j - r_i\right|^2}{w\left(\left|r_j - r_i\right|\right)}. \tag{7}$$

The pressure Poisson equation is obtained as follows:

$$< \nabla^2 P^{n+1} >= -\frac{\rho}{\Delta t^2} \frac{< n^* >_i - n^0}{n^0}. \tag{8}$$

The pressure Poisson equation can be solved with the incomplete Cholesky conjugate gradient method (ICCG).

In each step of simulation, use the initial number density n^0 and the number density n^* to set the pressure Poisson equation, and then obtained the pressure of the next step of simulation. Finally, the new velocities and position coordinates of the next step are obtained by adding the pressure gradient terms with the next step pressure values. With the correction velocities, the new velocities $\boldsymbol{v}_i^{n+1}$ and position coordinates r_i^{n+1} of the next step of simulation are obtained:

$$\boldsymbol{v}_i^{n+1} = \boldsymbol{v}_i^* - \frac{\Delta t}{\rho} \nabla p^{n+1}; \tag{9}$$

$$r_i^{n+1} = r_i^n + \Delta t \cdot v_i^{n+1}. \tag{10}$$

In the MPS method, the identification of the free surface is relatively simple, when the density of the particle population $< n^* >_i$ satisfies:

$$< n^* >_i < \beta n^0. \tag{11}$$

That particle is determined as the free surface particle. When solving the pressure Poisson equation, the zero boundary condition for the pressure is applied on those free surface particles. The parameter β is usually taken as 0.97, and n^0 is the initial particle number density which can be obtained by Eq. (4) in the initial step of the simulation.

2.2 The governing equations of elastomer

The governing equation of elastomer is as follows:

$$\rho \frac{\mathrm{D}v_\alpha}{\mathrm{D}t} = -\frac{\partial p}{\partial x_\alpha} + \frac{\partial \sigma_{\alpha\beta}}{\partial x_\beta}, \tag{12}$$

where,

$$p = -\lambda \varepsilon_{rr}; \tag{13}$$

$$\sigma_{\alpha\beta} = 2\mu \varepsilon_{\alpha\beta}; \tag{14}$$

$$\lambda_s = \frac{E\upsilon}{(1+\upsilon)(1-2\upsilon)}; \tag{15}$$

$$\mu = \frac{E}{2(1+\upsilon)}, \tag{16}$$

where ρ is the material density, p is the isotropic pressure which is obtained based on the particle location, $\sigma^{\alpha\beta}$ is the anisotropic stress tensor, λ_s and μ are the Lame constants, E is the Young modulus, and υ is the Poisson ratio.

$$\sigma_{ij} = 2\mu\varepsilon_{ij}^{n} = \frac{2\mu(u_{ij}\cdot r_{ij})r_{ij}}{\left|r_{ij}^{0}\right|\left|r_{ij}\right|^{2}}; \tag{17}$$

$$\tau_{ij} = 2\mu\varepsilon_{ij}^{s} = 2\mu\frac{u_{ij}}{\left|r_{ij}^{0}\right|} - \sigma_{ij}; \tag{18}$$

$$p = -\lambda(\varepsilon_{rr})_i = -\lambda\frac{d}{n^0}\sum_{j\neq i}\frac{u_{ij}\cdot r_{ij}}{\left|r_{ij}^{0}\right|\left|r_{ij}\right|}w\left(\left|r_{ij}^{0}\right|\right), \tag{19}$$

where σ_{ij} and τ_{ij} are the Normal stress and shear stress to particles i and j, and p is an isotropic pressure which is obtained based on the particle location, and u_{ij} is the variation of the relative position between the particles.

The acceleration produced by the force between the particles is:

$$\left[\frac{\partial v_i}{\partial t}\right]_{\mathrm{n}} = \frac{2d}{\rho_i n^0}\sum_{j\neq i}\frac{\sigma_{ij}}{\left|r_{ij}^{0}\right|}w\left(\left|r_{ij}^{0}\right|\right); \tag{20}$$

$$\left[\frac{\partial v_i}{\partial t}\right]_{\mathrm{s}} = \frac{2d}{\rho_i n^0}\sum_{j\neq i}\frac{\tau_{ij}}{\left|r_{ij}^{0}\right|}w\left(\left|r_{ij}^{0}\right|\right); \tag{21}$$

$$\left[\frac{\partial v_i}{\partial t}\right]_{\mathrm{p}} = -\frac{d}{\rho_i n^0}\sum_{j\neq i}\frac{(p_i+p_j)r_{ij}}{\left|r_{ij}^{0}\right|\left|r_{ij}\right|}w\left(\left|r_{ij}^{0}\right|\right), \tag{22}$$

$\left[\frac{\partial v_i}{\partial t}\right]_{\mathrm{s}}$ is the shear acceleration, $\left[\frac{\partial v_i}{\partial t}\right]_{\mathrm{n}}$ is the normal acceleration, $\left[\frac{\partial v_i}{\partial t}\right]_{\mathrm{p}}$ is the acceleration produced by the pressure.

$$v_i^{n+1} = v_i^{n} + \Delta t\left[\frac{\partial v_i}{\partial t}\right]^{n}; \tag{23}$$

$$r_i^{n+1} = r_i^{n} + \Delta t v_i^{n+1}. \tag{24}$$

2.3 Numerical simulation process

The MPS method is adopted to deal with the fluid–structure coupling problem. Firstly, ignore the properties of the solid particles. They are treated as fluid particles, and the MPS method can also be adopted for all particles. The speed and position of solid particles are updated in accordance with elastomer governing equation. The specific simulation process is shown in Fig. 1. When the LES method is used to simulate the turbulent flow, the fluid governing equation should be added up with sub-grid Reynolds stressing force item F_{sps} compared with Eq. (2). This sub-grid Reynolds stressing force item should be written as the following two equations:

$$F_{\mathrm{sps}x} = \frac{\partial}{\partial x}\left(2\nu_{\mathrm{t}}\frac{\partial\bar{u}}{\partial x} - \frac{2}{3}k\right) + \frac{\partial}{\partial y}\left[\nu_{\mathrm{t}}\left(\frac{\partial\bar{u}}{\partial y} + \frac{\partial\bar{v}}{\partial x}\right)\right]; \tag{25}$$

$$F_{\mathrm{sps}y} = \frac{\partial}{\partial x}\left[\nu_{\mathrm{t}}\left(\frac{\partial\bar{u}}{\partial y} + \frac{\partial\bar{v}}{\partial x}\right)\right] + \frac{\partial}{\partial y}\left(2\nu_{\mathrm{t}}\frac{\partial\bar{v}}{\partial y} - \frac{2}{3}k\right), \tag{26}$$

where $F_{\mathrm{sps}x}$ and $F_{\mathrm{sps}y}$ are the components of sub-grid Reynolds stressing force item in the direction of x and y. The simulation sequence of the MPS-LES is consistent with the simulation sequence of the ordinary MPS method. The distinction is that the sub-grid Reynolds stressing force should be considered together with the volume force and boundary conditions of the fluid particles, as shown in the below equation:

$$\Delta\boldsymbol{v}_i^{*} = \boldsymbol{v}_i + (\upsilon\nabla^2\boldsymbol{v}_i + F + F_{\mathrm{sps}})\cdot\Delta t. \tag{27}$$

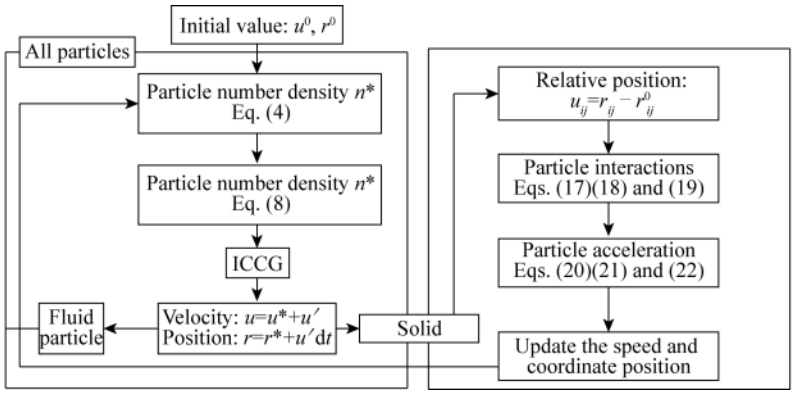

Fig. 1. Algorithm of MPS simulation.

In Eq. (27), Δv_i^{*} is an intermediate speed value, Δt is the time increment. The other parts of the process are consistent with the general MPS algorithms. The rest of the process is consistent with the general MPS algorithms.

In some steps of the simulation, a few of the particles were too close and even passed through the solid boundary, which could not happen in reality. Therefore, an additional modification was added after correcting the coordinates, by choosing a distance parameter. If two particles are too close ($r_{ij} < 0.025l_0^2$, l_0 is the spacing of particles), they are pulled

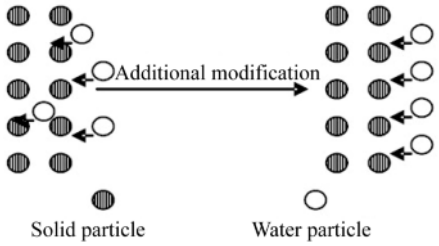

Fig. 2. Additional modification step.

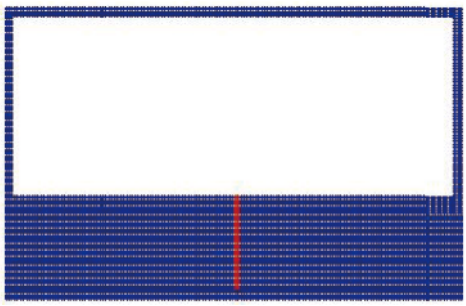

Fig. 3. Clamped elastic beam immersed in oil flow.

away by this additional modification.

Fluid particle updates its position with a modified velocity given by the method of weighted average, and then the probability of crossing is reduced. In practice, good results are obtained with this method. When a fluid particle and a solid particle are too close, the velocity and position of the fluid particle are updated based on Eq. (28) and Eq. (29).

$$v_j = v_j + v_r/\rho_j; \tag{28}$$

$$x_j = x_j + \mathrm{d}t \cdot v_r/\rho_j, \tag{29}$$

in which v_r can be written as:

$$v_r = \rho_i\left(v_i - v_g\right). \tag{30}$$

And the average velocity of two particles v_g is derived by Eq. (31)

$$v_g = \left(\rho_i v_i + \rho_j v_j\right)\Big/\left(\rho_i + \rho_j\right). \tag{31}$$

3 Results of the numerical simulation

3.1 Calculation condition

These cases consist of a rectangular container partially filled with oil. This fluid interacts with a flexible structure which is clamped to the bottom of the tank. The container rotates around the mid-point of its bottom. The width of the tank is 0.609 m and the height is 0.345 m. The liquid level is 0.115 m. The baffle is in the middle of the tank. The thickness of the elastic baffle is 0.004 m. The flat elastic modulus is set as 4.0×10^6 Pa, and the density is 1.1 times than that of water. The tank is forced to roll with the motion as follows:

$$\theta = \theta_{\max}\sin(2\pi t/T), \tag{32}$$

where θ is the roll angle of the tank, $\theta_{\max}$, and the maximum angle $\theta_{\max} = 4°$. The roll period T=1.4 s, and the density of oil is 0.917 times that of water. The results are shown in Fig. 3, the particle spacing $l_0 = 0.004$ m, $r_e = 2.1l_0$, and the time step is set as 0.00003 s in the numerical simulation.

3.2 Comparison between the experimental and numerical simulation results

When suffering from external excitations, the liquid in the tank will be forced to slosh and the FSI between elastic baffle and liquid appears under the effect of sloshing loads. Snapshots of the experiment (Idelsohn et al., 2008a, 2008b) are shown and compared with the MPS-FSI results at the same times in Fig. 4. In sloshing, the baffle produces a significant elastic deformation. It is very difficult for the traditional mesh method to simulate this kind of problem, because too much mesh deformation results in distortion, and grid computing terminates. The improved MPS method based on the LES can accurately simulate the large deformation of fluid free surface which is accompanied with the breaking, splashing and elastic deformation of elastic baffle under the impact of fluid. The agreement between results of the experiment and those of the MPS-FSI with LES is acceptable.

During the rolling excitation, the liquid interacts with elastic baffle so that the elastic baffle generates elastic deformation. During the deformations, the baffle applies the hinder force on the liquid and absorbs the energy and then has the effect of passive vibration reduction. The deformation history of the free end of the baffle is shown in Fig. 5. It can be seen that the deformation curve of the free end is similar to a sinusoid. As can be seen from Fig. 5, compared with the results of the particle finite element method (PFEM), the results of the MPS-FSI method agree better with the experimental results (Idelsohn et al., 2008a, 2008b). This is because the PFEM method (Idelsohn et al., 2008a, 2008b) will affect the computational accuracy on account of the excessive distortion of the grid when calculating the large deformation problem of the FSI. However, the MPS-FSI method is a pure Lagrange particle method which replaces the mesh with particles and completely gets rid of the constraints of the computational mesh. Thus, compared with the traditional mesh method, this method has obvious advantages in dealing with the large deformation of the structure.

Convergence has always been an important problem of the numerical calculation. It shows the rationality of the numerical solution. This section will be the convergence analysis of the MPS-FSI method based on the time step. In order to verify the influence of the time step on the calculation results, different time steps are adopted for calculation. The time step is set as Case 1 (2e–5 s), Case 2 (3e–5 s) and Case 3 (4e–5 s), respectively. The deformation history of

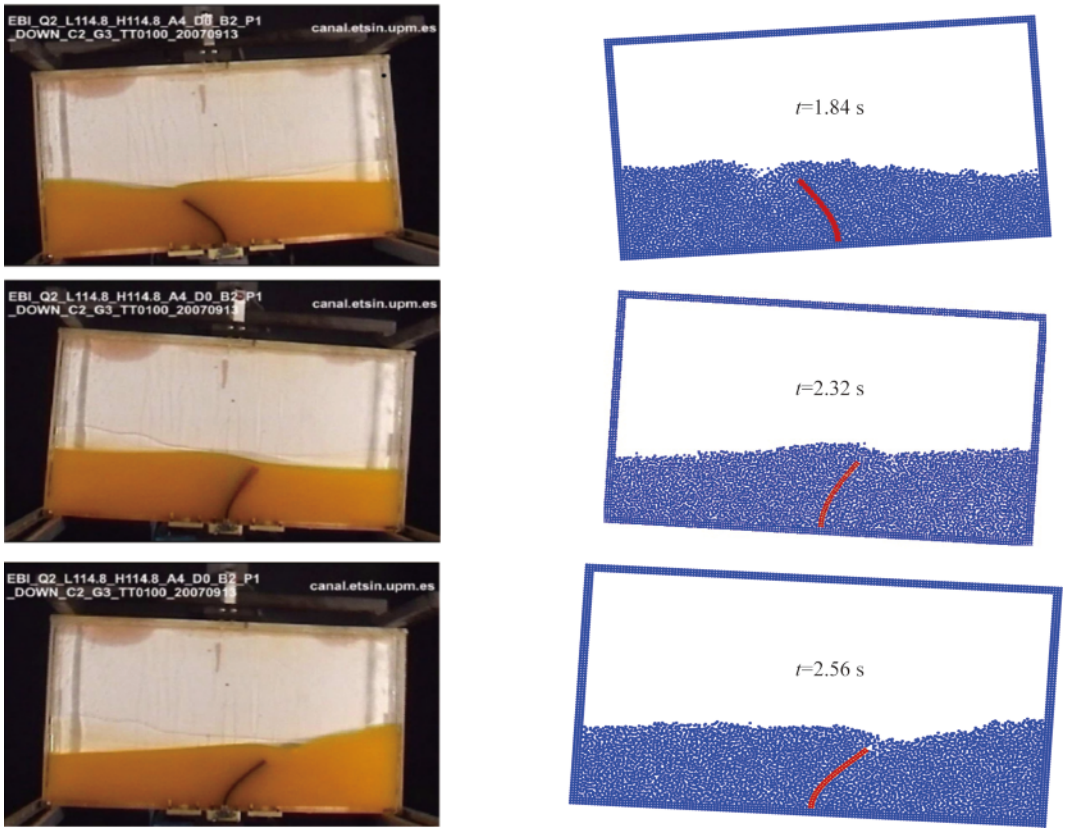

Fig. 4. Clamped elastic beam in oil.

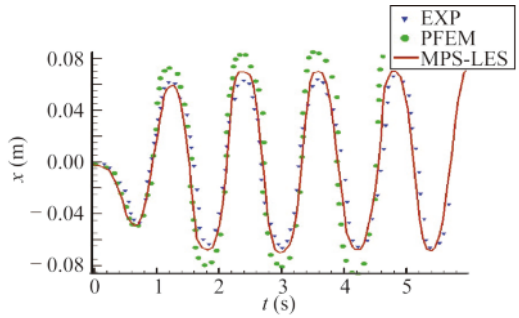

Fig. 5. Comparison of the displacement in the x direction.

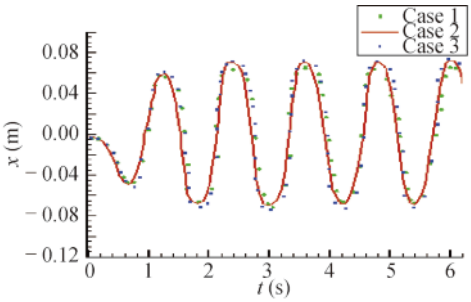

Fig. 6. Comparisons of numerical results obtained with different time steps.

the free end of the baffle is shown in Fig. 6, as can be seen, different time steps have little effect on the results of the MPS-FSI so that those results keep remarkable consistency.

The results of three other simulations corresponding to initial particle spacing of $l_0 = 0.004$, $l_0 = 0.002$ and $l_0 = 0.001$ are also shown to check the convergence. It can be seen from Fig. 7 that the particle spacing has no great influence on the calculation results, and the results of the three cases are almost the same. Thus, the numerical results of this method are stable and reliable.

3.3 Influence of the LES on sloshing

The simulation is carried out on sloshing in a tank with elastic baffle, according to the viscous laminar flow and turbulence flow, respectively. The deformation histories of the baffle free end are shown in Fig. 8, where MPS-VL represents MPS-Viscous Laminar Flow. From that figure, it can be seen that two curves basically coincide, but the difference appears only at the crest and trough. Because the MPS-VL only considers the viscosity of the fluid, while the MPS-LES considers the eddy-viscosity in addition.

The wave heights calculated at the right bulkhead from both the MPS-VL and MPS-LES are compared and their histories are shown in Fig. 9. As can be seen from that figure, in both methods, the tank suffers the severe sloshing, the flow climbs up at the bulkhead and wave height curve is periodic. However, the amplitude obtained from the MPS-LES is obviously larger than that from the MPS-VL, because the fluid moves more violently in turbulence, which

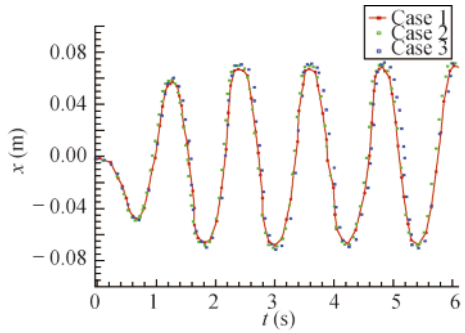

Fig. 7. Comparisons of the numerical results obtained with different particle spacing.

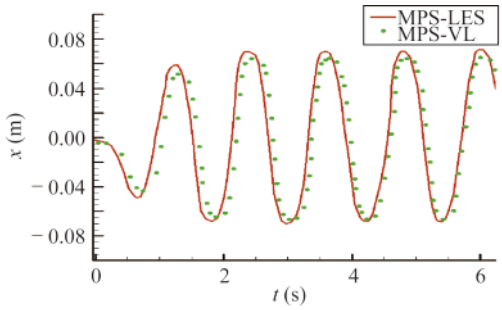

Fig. 8. Comparisons of the displacement obtained with different models.

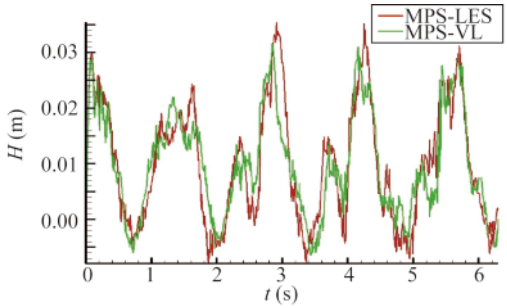

Fig. 9. Comparisons of the wave height obtained with different models.

leads to the larger wave amplitude.

3.4 Comparison of the numerical simulations between the ordinary tank and the one with a baffle

According to Fig. 10, it can be seen that the partition plate has favorable damping effect on sloshing. When a partition plate is not set in the tank, liquid sloshes fiercely and even hits the top of the tank, which means the sloshing liquid has great impact effect on the tank. Meanwhile, due to the severe deformation of the free surface, the complex flowing phenomenon such as wave curling, wave breaking and splashing may happen. However, after the partition baffle is set, sloshing is reduced obviously without hitting the top of the tank and the free surface is smoother. That is due to the reason that the partition baffle hinders the liquid motion and decreases the kinetic energy.

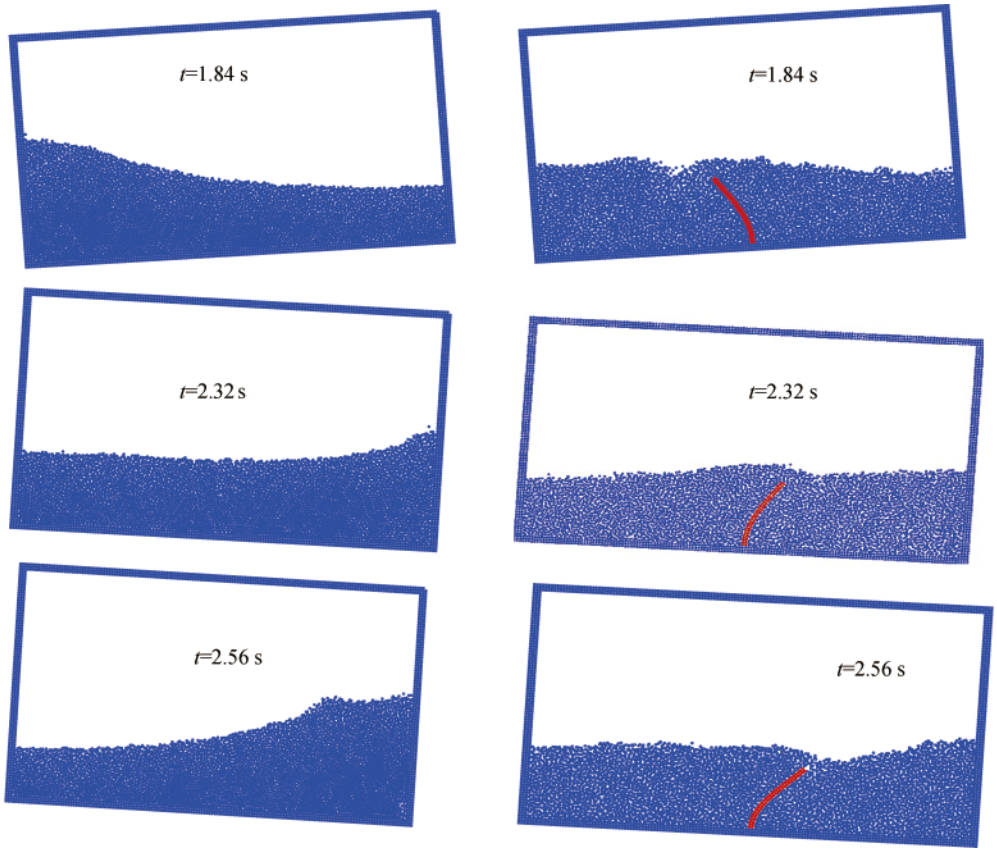

Fig. 10. Comparison of the numerical results.

This paper contrasts the wave amplitude at the right bulkhead of an ordinary tank with that of a tanker containing an elastic baffle, and the amplitude histories are displayed in Fig. 11. As shown, the two cases have basically the same period. However, in the ordinary tank without any baffle, the behavior of sloshing is violent and thus has larger amplitude at the peak. Whereas once the baffle is set, sloshing is obviously restrained. Hence, the elastic baffle has a great dissipation effect on sloshing.

Fig. 12 shows the histories of original pressure acting on the right bulkhead which can be seen from the figure that the pressure at the point oscillates very much. This problem occurs mainly due to the MPS method algorithm itself. Other reasons are random selection of the kernel function, the free surface of determination and particle motion.

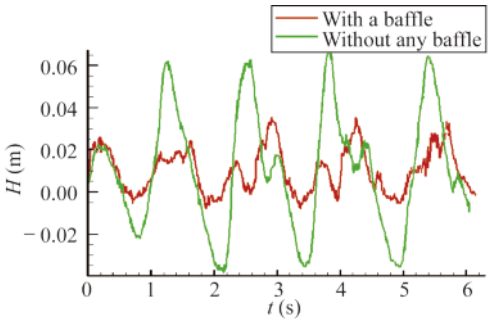

Fig. 11. Curves of the wave height at the right bulkhead.

In computational fluid dynamics, fluid compressibility can be guaranteed by limiting the velocity divergence to be zero. Substitute the condition into the pressure Poisson equation. Then the relation between pressure and velocity is obtained:

$$\nabla^2 P = \frac{\rho}{\Delta t}\nabla \cdot v^*. \tag{33}$$

Substituting Eq. (28) and the original number density into the Posisson equation at the same time, the improved pressure Poisson equation is obtained:

$$< \nabla^2 P^{n+1} >= \frac{\rho}{\Delta t}\nabla \cdot v^* - \gamma \frac{\rho}{\Delta t^2}\frac{< n^* >_i - n^0}{n^0}, \tag{34}$$

where γ is the relaxation factor, which can be fixed to obtain better results according to different calculation conditions.

After the pressure correction, the curve shown in Fig. 13 indicates that the pressure oscillation is within the acceptable range. During the sloshing, the momentum of fluid changed instantaneously due to the hindering effect of the tank, which then generates the slamming effect on the bulkhead. After a partition baffle being set inside the tank, the time-pressure curve approaches to sine curve and the amplitude of the slamming pressure peaks reduces largely. Because the decreased speed of the sloshing liquid by the partition plate has much less fluid kinetic energy and then the slamming pressure of sloshing on the wall is reduced seriously.

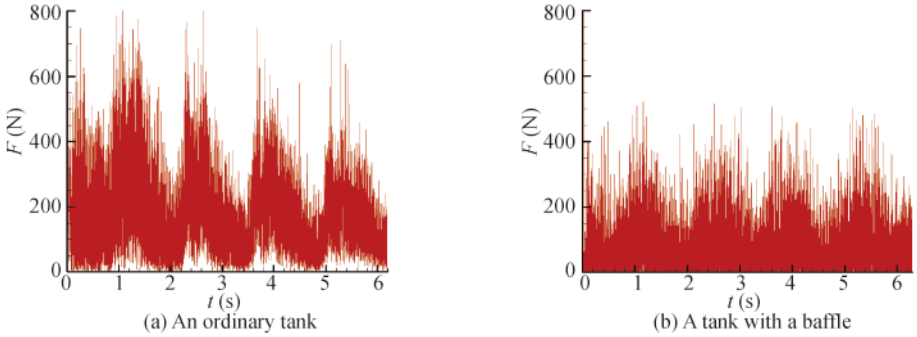

Fig. 12. Original pressure histories.

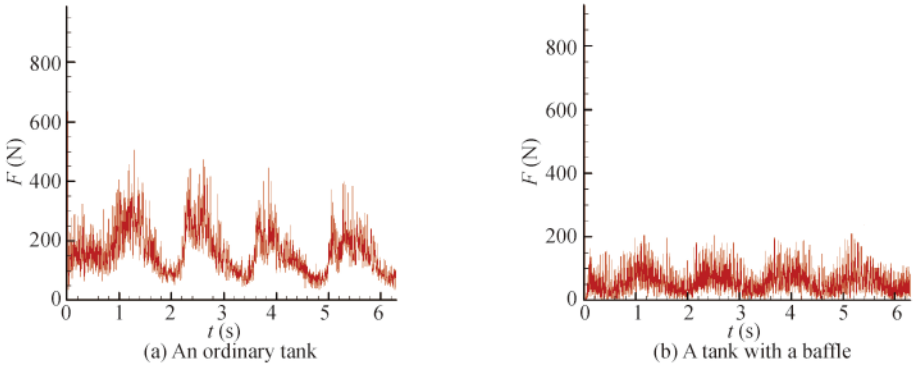

Fig. 13. Improved pressure histories.

3.5 Simulation for damaging the baffle

It is easy for the partition baffle to be damaged due to the severe deformation, although the baffle can reduce the amplitude of the free surface in sloshing and the pressure on the tank. But it is difficult for the traditional mesh methods to simulate the damaging of the partition baffle because of some effect factors such as the mesh distortion, etc. Whereas the MPS as a meshless method has an advantage for the damaging problems.

Kernel function $w(r)$ is the basis for all other MPS models, which is essentially the force function of the particles with neighbors. The value of the kernel function is determined by the distance between the particles. When the elastic structure deformed, the value of the kernel function between the particles will also change. This paper assumes that if the strain exceeds $\delta = \frac{l - l_0}{l_0} \geqslant 0.05$, and $w(r)=0$, then the elastic structure is damaged. The simulation carried out on the damage of the baffle pays more attention to the validation of theoretical method but the research on realistic materials will be the principal focus of the future work.

The partition baffle damage under the MPS simulation is shown in Fig. 14. Fig. 14 indicates that the bottom of the elastic baffle is damaged and the baffle is integrity collapsed given E=5.0×10^5 Pa.

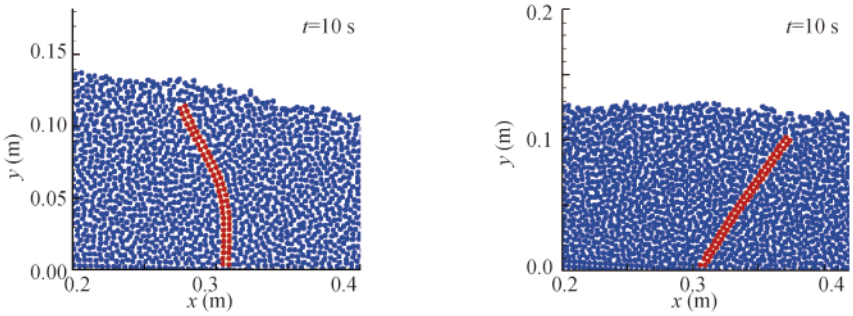

Fig. 14. Simulation for damaging the baffle using the MPS method (E=5.0×10^5 Pa)

The failure of the plate simulated by the MPS method is verified. According to the research of Cao (2009), similar to the cantilever plate, the first damage occurs at the fixed end of the plate under the impact of water flow. The location of the damage point x_0 is calculated according to the following formula. When $l_1 < 2.2h_b$, $x_0 = 0.13l_1$. l_1 is the height of the fixed end, and h_b is the thickness of the plate. This paper sets the bottom of the particle with a fixed end and the height of 0.004. By calculations, the plates first break down at the bottom and the last second particles. From Fig. 14, the numerical simulation results of the damage locations are consistent with the theoretical results, so the numerical simulation results are authentic. Traditional numerical methods always fail in dealing with such kinds of corruption problems due to excessive deformation of the grids. On the contrary, MPS method is much easier and efficient in calculating these corruption problems because of its particle properties.

4 Conclusions

It is very difficult for the traditional mesh method to simulate sloshing problems due to such reasons as the splashing of the free surface, the large deformation of the partition baffle and the strict requirements on the mesh when damages occur. Whereas the MPS method gets rid of the constraints of grids completely and discards the remeshing process. Consequently, the MPS-FSI method has significant advantages in handling the discontinuity at the interface in the FSI.

In this paper, the FSI of the sloshing model is simulated using the moving particle semi-implicit method with LES.

(1) The improved MPS method can accurately simulate the large deformation of the free surface even with breaking and splashing as well as the deformation of the elastic baffle under the impact of the fluid. The numerical results are in good agreement with the experimental ones.

(2) The wave amplitude calculated from the MPS-LES is obviously larger than that from the MPS-VL, due to the fact that the fluid moves more violently in turbulence. Besides, the increase of the baffle elastic modulus plays a good role in restraining sloshing.

(3) In the tanker without any baffle, violent sloshing leads to strong flow hitting the top. The elastic baffle has a great effect on restraining sloshing and therefore reduces the pressure peaks at the bulkhead. And the pressure oscillation is markedly reduced after improving the Poisson pressure equation.

(4) The idea of the Lagrangian particle in the MPS results in the promising application in the damage calculations. This paper has carried out theoretical research on applying the MPS-FSI method to the calculations of the structural damage and demonstrated the feasibility.

References

Abramson, H.N., 1966. *The Dynamic Behavior of Liquids in Moving Containers*, NASA Report, SP 106.

Biswal, K.C., Bhattacharyya, S.K. and Sinha, P.K., 2006. Nonlinear sloshing in partially liquid filled containers with baffles, *International Journal for Numerical Methods in Engineering*, 68(3), 317–337.

Cao, T.J., 2009. Analysis to large deflections of elastic cantilever beam with constraint under uniformly distributed load, *Journal of Civil Aviation University of China*, 27(5), 23–27. (in Chinese)

Chikazawa, Y., Koshizuka, S. and Oka, Y., 2001. A particle method for elastic and visco-plastic structures and fluid–structure interactions, *Computational Mechanics*, 27(2), 97–106.

Cho, J.R. and Lee, H.W., 2004. Numerical study on liquid sloshing in baffled tank by nonlinear finite element method, *Computer Methods in Applied Mechanics and Engineering*, 193(23–26), 2581–2598.

Dunne, T. and Rannacher, R., 2006. Adaptive finite element approximation of fluid–structure interaction based on an eulerian variational formulation, *Fluid–Structure Interaction Lecture Notes in Computational Science and Engineering*, 53, 110–145.

Gingold, R.A. and Monaghan, J.J., 1977. Smoothed particle hydrodynamics: Theory and application to non-spherical stars, *Monthly Notices of the Royal Astronomical Society*, 181(3), 375–389.

Gotoh, H., Shibahara, T. and Sakai, T., 2001. Sub-particle-scale turbulence model for the MPS method-Lagrangian flow model for hydraulic engineering, *Advanced Methods for Computational Fluid Dynamics*, 9(4), 339–347.

Idelsohn, S.R., Marti, J., Limache, A. and Oñate, E., 2008a. Unified Lagrangian formulation for elastic solids and incompressible fluids: Application to fluid-structure interaction problems via the PFEM, *Computer Methods in Applied Mechanics and Engineering*, 197(19–20), 1762–1776.

Idelsohn, S.R., Marti, J., Souto-Iglesias, A. and Oñate, E., 2008b. Interaction between an elastic structure and free-surface flows: Experimental versus numerical comparisons using the PFEM, *Computational Mechanics*, 43(1), 125–132.

Jung, J.J., Lee, H.H., Park, T.H. and Lee, Y.W., 2008. Experimental and numerical investigation into the effects of fluid–structure interaction on the sloshing impact loads in member LNG carrier, *Proceedings of the 27th International Conference on Offshore Mechanics and Arctic Engineering*, ASME, Estoril, Portugal, Paper No. OMAE2008-57323, pp. 665–671.

Kim, Y., 2001. Numerical simulation of sloshing flows with impact load, *Applied Ocean Research*, 23(1), 53–62.

Koshizuka, S. and Oka, Y., 1996. Moving-particle semi-implicit method for fragmentation of incompressible fluid, *Nuclear Science and Engineering*, 123(3), 421–434.

Koshizuka, S., Tamako, H. and Oka, Y., 1995. A particle method for incompressible viscous flow with fluid fragmentation, *Journal of Computational Fluid Dynamics*, 4, 29–46.

Liao, K.P. and Hu, C.H., 2013. A coupled FDM-EM method for free surface flow interaction with thin elastic plate, *Journal of Marine Science and Technology*, 18(1), 1–11.

Lucy, L.B., 1977. A numerical approach to the testing of the fission hypothesis, *Astronomical Journal*, 82(12), 1013–1024.

Okamoto, T. and Kawahara, M., 1990. Two-dimensional sloshing analysis by Lagrangian finite element method, *International Journal for Numerical Methods in Fluids*, 11(5), 453–477.

Pan, X.J., Zhang, H.X. and Sun, X.Y., 2012. Numerical simulation of sloshing with large deforming free surface by MPS-LES method, *China Ocean Engineering*, 26(4), 653–668.

Yu, Q. and Zhang, H.X., 2013. Research on water entry of wedge based on the improved MPS method with large eddy simulation, *The Ocean Engineering*, 31(6), 9–15, 90. (in Chinese)